Quantum tricritical point emerging in the spin-boson model with two dissipative spins in staggered biases

Yan-Zhi Wang,[1,2] Shu He,[3] Liwei Duan,[1,4] and Qing-Hu Chen[1,5,*]

[1]*Zhejiang Province Key Laboratory of Quantum Technology and Device, Department of Physics, Zhejiang University, Hangzhou 310027, China*

[2]*School of Physics and Electronic information, Anhui Normal University, Wuhu 241002, China*

[3]*Department of Physics and Electronic Engineering, Sichuan Normal University, Chengdu 610066, China*

[4]*Department of Physics, Zhejiang Normal University, Jinhua 321004, China*

[5]*Collaborative Innovation Center of Advanced Microstructures, Nanjing University, Nanjing 210093, China*

(Received 17 December 2020; accepted 23 April 2021; published 4 May 2021)

We study the spin-boson model (SBM) with two spins in staggered biases by a numerically exact method based on variational matrix product states. Several observables such as the magnetization, the entanglement entropy between the two spins and the bosonic environment, the ground-state energy, as well as the correlation function for two spins are calculated exactly. The characteristics of these observables suggest that the staggered biases can drive the second-order quantum phase transition (QPT) to the first-order QPT in the sub-Ohmic SBM, while the Kosterlitz-Thouless QPT in the Ohmic SBM goes directly to the first-order one. A quantum tricritical point, where the continuous QPT meets the first-order one, can then be detected. It is found that the staggered biases would not change the universality of the phase transition in this model below the quantum tricritical point.

DOI: 10.1103/PhysRevB.103.205106

I. INTRODUCTION

In the light-matter interacting systems, it is well known for a long time that the prototype Dicke model [1] and the spin-boson model (SBM) [2–4] can display quantum phase transitions (QPTs) at strong coupling between the two-level systems (qubits) and the cavity or the bosonic baths. Recently, it has even been proposed that the quantum Rabi model only consisting of one qubit and a single-mode cavity can undergo a QPT in the infinite ratio of the qubit and cavity frequencies [5], which further inspires a surge of studies for the so-called finite-component QPT [6–10]. It is generally accepted that the Dicke model and the quantum Rabi model only experience a single QPT from the normal to the superradiant phase with the same critical behavior, and the SBM exhibits the single QPT from the delocalized to the localized phases with the spectra function dependent critical exponents [11].

Theoretically, to obtain a rich phase diagram of quantum phases in the light-matter interacting systems, one can generalize these prototype models to their variants. Generally, the QPT only appears in the Dicke model in the thermodynamic limit, i.e., the qubit number $N \to \infty$, exhibiting the mean-field critical behavior. The generalized Dicke models, such as the anisotropic Dicke model [12–14], the anisotropic Dicke model with the nonlinear Stark coupling terms [15], and the Dicke model where infinite atoms are separated equally into two parts each experiencing the opposite equal biases [16] have been recently studied by several groups. In these generalized Dicke models, both the first- and second-order QPTs are observed. More recently, the existence of the finite-component multicriticality is demonstrated in a generalized Dicke model with a finite number of atoms at an extremely large detuning [17].

A quantum tricritical point (QuTP) [18] is seldomly supported in the solid-state materials and is almost impossible to appear in the prototype models of the light-matter interacting systems. Interestingly, it has been found to exist in anisotropic Dicke model [13] and the isotropic Dicke model with staggered biases [16]. In the former model, the QuTP lies at the symmetric line of the superradiant "electric" and "magnetic" phases, which can be mapped mutually by interchanging the rotating-wave term and the counterrotating one, while in the latter model, it was demonstrated that the field can drive the second-order QPT to the first-order one, thus the second-order critical line can meet the first-order critical line at the QuTP [16].

In the SBM with single qubit, the second-order QPT from the delocalized phase, where spin has equal probability in the two states, to the localized phase, in which the spin prefers to stay in one of the two states, has been studied extensively [11,19–30]. Recently, the anisotropic sub-Ohmic SBM has also been studied by the present authors [31]. It is generally accepted that the continuous QPT with mean-field exponents is found for the power of the bath spectral function $s < 1/2$ [19,20,22], with nontrivial exponents for $1/2 < s < 1$ [11,21]. The Kosterlitz-Thouless (KT) phase transition occurs for $s = 1$ [2], and no phase transition happens for $s > 1$.

The SBM has been generalized by increasing the number of spins, such as the SBM with two spins [32,33], and a finite number of spins even in the limit $N \to \infty$ [34]. It has been found that the critical behavior of QPT is not changed with

*Corresponding author: qhchen@zju.edu.cn

the increasing number of spins. Only in the limit $N \to \infty$, the universality class of the transition changes into mean-field behavior.

We will study the criticality of the generalized SBM with two spins in staggered biases. Our goals are twofold. Since the staggered biases result in the QuTP in the generalized Dicke model [16] and even multicriticality in a finite number of qubits collectively coupled to a single mode cavity at an extremely large detuning [17], we first explore whether the QuTP can emerge in the two-qubit SBM with staggered biases. In the original SBM, the continuous QPT occurs in the sub-Ohmic baths [11,19–22,24] where the critical exponents are bath dependent, while the KT phase transitions in the Ohmic bath [2,35]. This picture is not changed for the SBM with a finite number of spins without biases [32–34]. We then examine whether the presence of the staggered biases would change the universality class of these continuous QPTs in the SBM with two spins.

In this paper, we will extend the variational matrix product state (VMPS) approach [24] to study the two-spin-boson model (2SBM) with both sub-Ohmic and Ohmic baths. The paper is organized as follows. In Sec. II, we introduce the 2SBM in the staggered biases for two spins along the opposite directions and the VMPS approach briefly. In Sec. III, we study the QPTs of the 2SBM in both sub-Ohmic and Ohmic baths with the staggered biases. For the sub-Ohmic bath, we choose two typical powers of the spectra function of the bath, which are, respectively, corresponding to the mean-field and interacting critical nature of the QPTs in the single SBM. The order parameter and the entanglement entropy between the two qubits and the bosonic bath are extensively calculated. The critical exponents for the order parameter are also analyzed. A QuTP separated by the second-order (KT type) critical lines and the first-order ones for the sub-Ohmic (Ohmic) baths are revealed by several independent evidences from different observables. Finally, we present a brief summary in the last section.

II. 2SBM WITH STAGGERED BIASES AND METHODOLOGIES

The 2SBM Hamiltonian can be written as (the reduced Planck constant is set $\hbar = 1$)

$$\hat{H} = \sum_{i=1,2} \frac{1}{2}\left(\Delta\sigma_i^z - (-1)^i\epsilon\sigma_i^x\right) + \sum_k \omega_k a_k^\dagger a_k + \frac{1}{2}\sum_k g_k(a_k^\dagger + a_k)\left(\sigma_1^x + \sigma_2^x\right), \quad (1)$$

where $\sigma_{i=1,2}^j$ $(j = x, y, z)$ are the Pauli matrices for spins 1 and 2, Δ is the qubit frequency, $(-1)^i\epsilon$ before σ_i^x represents the staggered biases along the x axis for the two spins, a_k $(a_k^\dagger)$ is the bosonic annihilation (creation) operator which can annihilate (create) a boson with frequency ω_k, and g_k denotes the coupling strength between the qubit and the bosonic bath, which is usually characterized by the power-law spectral density $J(\omega)$,

$$J(\omega) = \pi\sum_k g_k^2\delta(\omega - \omega_k) = 2\pi\alpha\omega_c^{1-s}\omega^s\Theta(\omega_c - \omega), \quad (2)$$

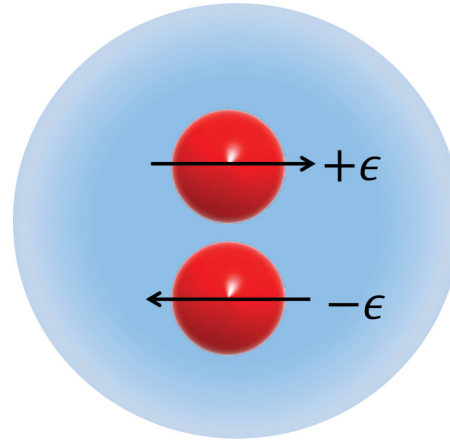

FIG. 1. Illustration of the two-spin-boson model with staggered biases $\pm\epsilon$ along the x direction. The two spins denoted by red spheres interact with a common continuous bosonic reservoir represented by the big blue region. No direct interaction between spins is considered.

where α is a dimensionless coupling constant, ω_c is the cutoff frequency, and $\Theta(\omega_c - \omega)$ is the Heaviside step function. The power of the spectral function s classifies the reservoir into super-Ohmic $(s > 1)$, Ohmic $(s = 1)$, and sub-Ohmic $(s < 1)$ types. This model is illustrated in Fig. 1 where the x axis is in a horizontal line.

The introduced staggered biases to the two spins do not break the parity (Z_2) symmetry in the 2SBM. The parity operator is defined as

$$\hat{\Pi} = \left[\frac{\sigma_1^z\sigma_2^z + 1}{2} - (\sigma_1^+\sigma_2^- + \sigma_1^-\sigma_2^+)\right]\exp\left(i\pi\sum_k a_k^\dagger a_k\right), \quad (3)$$

where $\sigma_{i=1,2}^{\pm} = (\sigma_i^x \pm i\sigma_i^y)/2$. Note that in the presence of the staggered biases, the parity operator is more complicated than that for $\epsilon = 0$, $\hat{\Pi}_{\epsilon=0} = \exp[i\pi(\sum_k a_k^\dagger a_k + (\sigma_1^z + \sigma_2^z)/2 + 1)]$, due to the absence of the collective spin. The parity operator $\hat{\Pi}$ has two eigenvalues ± 1, corresponding to the even and odd parity in the symmetry conserved phases. The average value of the parity may become zero due to the quantum fluctuations in the symmetry broken phase.

To apply VMPS in the 2SBM in staggered biases, the logarithmic discretization of the spectral density of the continuum bath [11] with discretization parameter $\Lambda > 1$ is performed first, followed by using orthogonal polynomials as described in Ref. [36], the 2SBM can be mapped into the representation of an 1D semi-infinite chain with nearest-neighbor interaction [37]. Thus, Hamiltonian (1) can be written as:

$$H_{\text{chain}} = \frac{\Delta}{2}\left(\sigma_1^z + \sigma_2^z\right) + \frac{\epsilon}{2}\left(\sigma_1^x - \sigma_2^x\right) + \frac{c_0}{2}(b_0 + b_0^\dagger)\left(\sigma_1^x + \sigma_2^x\right) + \sum_{n=0}^{L-2}[\varepsilon_n b_n^\dagger b_n + t_n(b_n^\dagger b_{n+1} + b_{n+1}^\dagger b_n)], \quad (4)$$

where $b_n^\dagger(b_n)$ is the creation (annihilation) operator for a new set of boson modes in a transformed representation with ε_n

describing the frequency on chain site n, t_n the nearest-neighbor hopping parameter, and c_0 the effective coupling strength between the spin and the new effective bath. For more details, one may refer to Ref. [36].

Then as introduced in Refs. [38,39], we employ the standard matrix product representation with the optimized boson basis $|\widetilde{n}_k\rangle$ through an additional isometric map with truncation number $d_{\rm opt} \ll d_n$ like in Refs. [24,37] to study the quantum criticality of 2SBM. Each site in the 1D chain can be described by the matrix M_s, which is optimized through sweeping the 1D chain iteratively to obtain the ground state, and D_n is the bond dimension for matrix M_s with the open boundary condition, bounding the maximal entanglement in each subspace.

For the data presented below, we typically choose the same model parameters in Refs. [24,31,40], as $\Delta = 0.1$, $\omega_c = 1$, the logarithmic discretization parameter $\Lambda = 2$, the length of the semi-infinite chain $L = 50$, and optimized truncation numbers $d_{\rm opt} = 12$. In addition, we adjust the bond dimension as $D_{\rm max} = 20$, 40, and 20 for $s = 0.3$, 0.7, and 1, respectively, which are sufficient to obtain the converged results for the problems concerned. Actually, the convergence thresholds for the bond dimensions are $D = 12$ for $s = 0.3$, and $D = 20$ for $s = 0.7$ and 1 for the all observables. Only in the critical regime, we use larger bond dimensions $D = 20$ for $s = 0.3$ and $D = 40$ for $s = 0.7$ to improve computational accuracy where the relative error is less than 10^{-7} for the energy and 10^{-5} for the magnetization, so that we can evaluate the critical exponents precisely. The evidence for the full convergence of our VMPS results here is similar to that demonstrated in the Appendix of Ref. [40] and will not be repeated in this paper.

The information of the ground state can also be described by the von Neumann entropy S_E of the 2SBM, which characterizes the entanglement between two spins and the bosonic bath

$$S_E = -Tr(\rho_{\rm spin} \log \rho_{\rm spin}), \tag{5}$$

where $\rho_{\rm spin}$ is the reduced density matrix for the two spins. The averaged total magnetization

$$M = \left(\langle\sigma_1^x\rangle + \langle\sigma_2^x\rangle\right)/2 \tag{6}$$

can be regarded as the order parameter, which can be used to characterize the essential nature of the second-order QPTs. However, M is hardly employed to distinguish the KT and the first-order QPTs, because it would suddenly drop to zero in both cases.

III. RESULTS AND DISCUSSIONS

A. Sub-Ohmic bath ($s < 1$)

The single SBM expects a mean-field critical behavior for $s < 1/2$ and a nonclassical one for $s > 1/2$, so we focus on two typical powers of the spectral function $s = 0.7$ and 0.3 for the sub-Ohmic case. The entire critical lines can be mapped out by the onset of the nonzero order parameter $M = (\langle\sigma_1^x\rangle + \langle\sigma_2^x\rangle)/2$. By this criterion, the phase diagrams of 2SBM with staggered biases are summarized in the $\epsilon - \alpha$ plane in the upper panels of Fig. 2 for $s = 0.3$ (left) and 0.7 (right), respectively. To confirm the phase diagram more convincingly, we also display the entanglement entropy S_E between the two spins and the bath, an alternative widely used

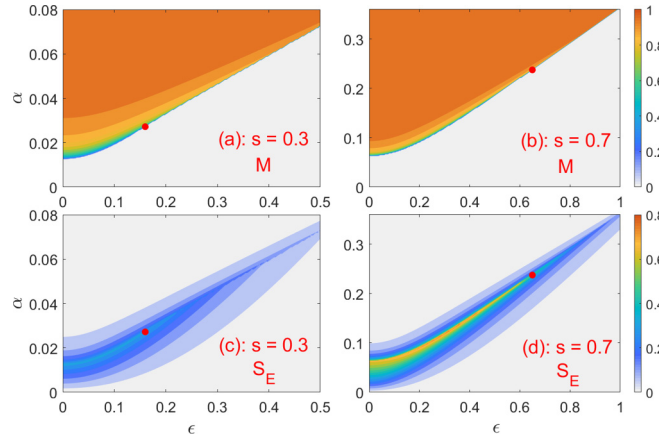

FIG. 2. (Upper panels) Phase diagram in the $\epsilon - \alpha$ plane for 2SBM drawn from the magnetization M: delocalized phases ($M = 0$) and the localized phase ($M \neq 0$). (Lower panels) Entanglement entropy S_E. The power of the spectral function is (left) $s = 0.3$ and (right) 0.7. $\Delta = 0.1$, $\omega_c = 1$. The QuTP is marked by a red dot, which separates the intersection of the second- and first-order phase transition. The parameters used in the VMPS approach are $\Lambda = 2$, $L = 50$, $d_{\rm opt} = 12$, and $D = 20$ for $s = 0.3$, 0.7.

tool in the location of QPTs, in the lower panels of Fig. 2. The entropy displays a sharp nonanalyticity at the phase transition [23,41,42]. The ridge line of S_E obviously shows a sharp nonanalyticity, which exactly coincides with the critical line obtained by the order parameter. At either infinite coupling strength or infinite bias, the entanglement becomes zero due to the decoupling of systems and environments in two extreme cases.

To explore the nature of QPTs with different staggered biases, we will discuss the order parameter and the entanglement entropy in detail. We extract the data of the order parameter and the entropy as a function of coupling strength α along $\epsilon = 0.1$, 0.2 for $s = 0.3$, and $\epsilon = 0.5$, 0.7 for $s = 0.7$, and replot in the upper panels of Figs. 3 and 4, respectively. It is found that the order parameter (blue line) becomes nonzero continuously for $\epsilon = 0.1$ at $s = 0.3$ and $\epsilon = 0.5$ at $s = 0.7$, indicating a second-order QPT, while it suddenly jumps to a finite value for $\epsilon = 0.2$ at $s = 0.3$ and $\epsilon = 0.7$ at $s = 0.7$, suggesting a first-order QPT. By extensive calculations in a similar way, we can immediately locate a critical point that splits the whole critical line into the first- and second-order critical lines, as indicated in the upper panels of Fig. 2 with red dots. This is just a QuTP, similar to that observed in the generalized Dicke model in the staggered biases [16].

The same picture can also be drawn from the entanglement entropy indicated with red lines in the upper panels of Figs. 3 and 4. For $\epsilon = 0.1$ at $s = 0.3$ and $\epsilon = 0.5$ at $s = 0.7$, the entropy of entanglement S_E displays a cusplike behavior, similar to that observed in the single sub-Ohmic SBM [23,42], thus demonstrating the second-order QPT. Whereas, for large ϵ, e.g., for $\epsilon = 0.2$ at $s = 0.3$ and $\epsilon = 0.7$ at $s = 0.7$, although the entropy still displays a sharp nonanalyticity at the transition point, it suddenly drops to a finite value, in contrast to the second-order QPT for small ϵ where S_E falls off gradually on both sides of the phase transition point. As shown in the

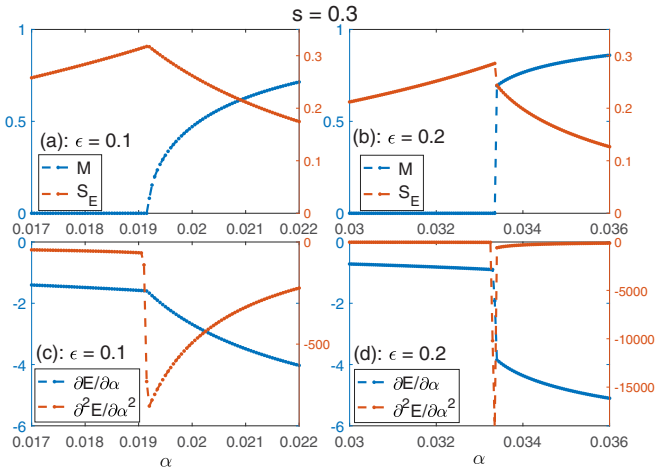

FIG. 3. Magnetization M, entanglement entropy S_E (upper panels), the first- and second-order derivatives of the ground-state energy (lower panels) as a function of α for $\epsilon = 0.1$ (left) and $\epsilon = 0.2$ (right) for the sub-Ohmic bath with $s = 0.3$ by VMPS approach. $\Delta = 0.1$, $\omega_c = 1$, $\Lambda = 2$, $L = 50$, $d_{\text{opt}} = 12$, and $D = 20$.

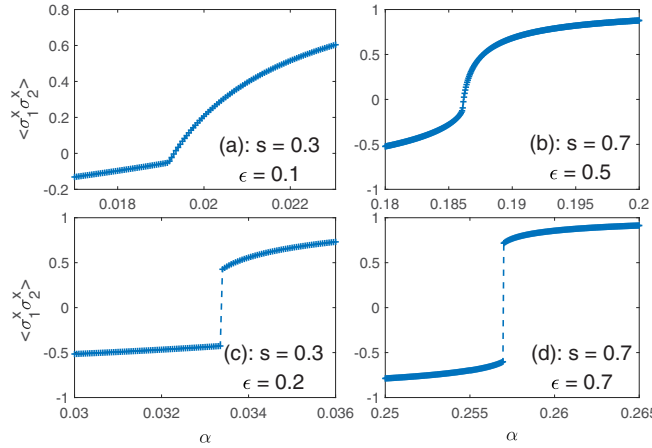

FIG. 5. The correlation function $\langle\sigma_1^x\sigma_2^x\rangle$ as a function of the coupling strength for the sub-Ohmic bath by VMPS approaches at $\epsilon = 0.1, 0.2$ for $s = 0.3$ (left) and $\epsilon = 0.5, 0.7$ for $s = 0.7$ (right). Other parameters: $\Delta = 0.1$, $\omega_c = 1$, $\Lambda = 2$, $L = 50$, $d_{\text{opt}} = 12$, $D = 20$.

upper left panels of Figs. 3 and 4, the sudden drop of the entropy occurs simultaneously at the sudden jump of the order parameter at the same ϵ, thus both suggesting the first-order QPTs.

The first-order and second-order QPTs can also be directly discerned by the first- and second-order derivatives of the ground-state energy with respect to the coupling parameter α. The results at the same model parameters are presented in the lower panels of Figs. 3 and 4. At the two smaller staggered bias (lower left), the first-order derivatives of the energy are continuous around the transitions, while at the two larger staggered biases (lower right), they are discontinuous at the critical points, whereas the second-order derivatives of energy are discontinuous for smaller ϵ and diverge for the larger ϵ at the phase transition points for each bath exponent

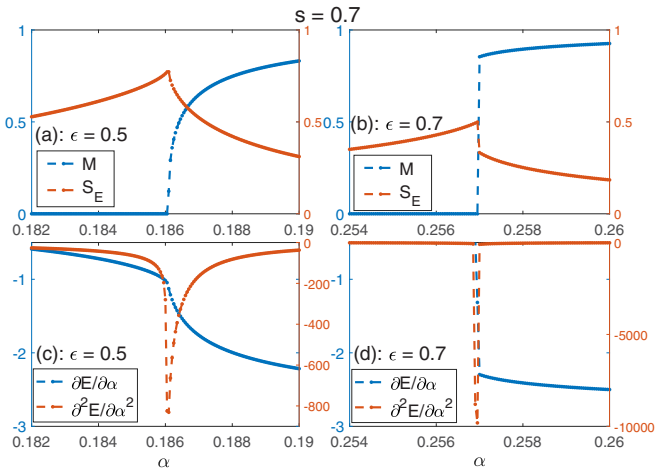

FIG. 4. Magnetization M, entanglement entropy S_E (upper panels), the first- and second-order derivatives of the ground-state energy (lower panels) as a function of α for $\epsilon = 0.5$ (left) and $\epsilon = 0.7$ (right) for the sub-Ohmic bath with $s = 0.7$ by VMPS approach. $\Delta = 0.1$, $\omega_c = 1$, $\Lambda = 2$, $L = 50$, $d_{\text{opt}} = 12$, and $D = 20$.

s, respectively. The observations based on the ground-state energy are obviously in accord with the original criterion of the second- and first-order phase transitions, justifying again the existence of QuTP in the phase diagram based on the order parameter and the entropy.

To provide further evidence of the existence of the QuTP separating the first- and second-order critical lines, we calculate the two spin correlation function $\langle\sigma_1^x\sigma_2^x\rangle$. The results are shown in Fig. 5 for $s = 0.3$ (left) and 0.7 (right), at small and large biases, which are the same as those in Figs. 3 and 4. It is observed that the $\langle\sigma_1^x\sigma_2^x\rangle$ is continuous (discontinuous) for small (large) staggered biases, also demonstrating the second- (first)-order QPTs at the corresponding bias.

Since the staggered biases can drive the second-order QPTs to the first-order ones, can it alter the universality class in the second-order critical lines? In order to answer this question, we present the log-log plot of the magnetization $M = (\langle\sigma_1^x\rangle + \langle\sigma_2^x\rangle)/2$ as a function of $\alpha - \alpha_c$ in Fig. 6 where the parameters are the same as those in Fig. 5. The critical exponents β can be determined by fitting power-law behavior, $M \propto (\alpha - \alpha_c)^\beta$. For two smaller biases below the QuTP, as displayed in the upper panels of Fig. 6, very nice power-law behavior over three decades is demonstrated for both cases, yielding $\beta = 0.484$ for $s = 0.3$ and $\beta = 0.303$ for $s = 0.7$, which are very close to those in the single SBM for the same s by the VMPS approaches [24]. This is to say, the critical exponents of the order parameter are not different from those in the single SBM. In other words, as long as the second-order QPTs occur in the 2SBM with the staggered biases, the critical exponent is only the bath dependent, and remains unchanged with ϵ. At the first-order critical line in the large ϵ regime, as shown in the low panels of Fig. 6, $\beta = 0$, consistent with the first-order phase transition nature.

B. Ohmic bath ($s = 1$)

It is well known that the single SBM with the Ohmic bath undergoes the continuous QPTs of KT type [2]. In the

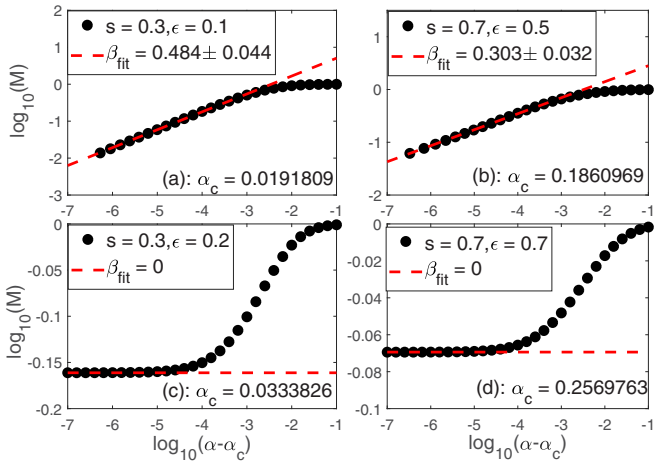

FIG. 6. The log-log plot of the magnetization M as a function of $\alpha - \alpha_c$ at $\epsilon = 0.1, 0.2$ for $s = 0.3$ (left panels) and $\epsilon = 0.5, 0.7$ for $s = 0.7$ (right panels). The numerical results by VMPS are denoted by black circles and the power-law fitting curves are denoted by the red dashed lines, which indicates the second-order QPT takes place in the smaller staggered biases and gives similar critical behaviors compared to the standard spin-boson model, while the larger staggered biases induce the first-order QPT and vanishing of the critical exponent β. $\Delta = 0.1$, $\omega_c = 1$, $\Lambda = 2$, $L = 50$, $d_{\text{opt}} = 12$, and $D = 20, 40$ for $s = 0.3, 0.7$, respectively.

language of the quantum-to-classical mapping, $s = 1$ corresponds to the low critical dimension of the long-ranged Ising model [43]. As shown in the last section, in the sub-Ohmic 2SBM, the staggered biases can drive the second-order QPT to the first-order one. Then what is the effect of these staggered biases on the KT phase transitions in the Ohmic 2SBM? Could the staggered biases drive the KT phase transitions to the second-order or/and the first-order ones? To address these issues, we also extend to study 2SBM in the Ohmic bath with the staggered biases using the VMPS in this subsection. In the literature, the entanglement entropy is usually studied in the SBM with the Ohmic bath, because KT phase transitions are of infinite order, and less observables can be used to distinguish KT from other kinds of phase transitions. In the KT phase transition of the single SBM for $s = 1$, the entropy increases in the weak coupling regime, then saturates to a plateau, and drops suddenly at the KT critical point [35]. The sudden drop of the entanglement entropy signifies the onset of an emergent new phase. In the second-order QPTs, the entropy falls off gradually on both sides of the critical point [23,42], displaying different behavior from those in both the KT and the first-order QPTs.

We calculate the entanglement entropy for several staggered biases from $\epsilon = 0$ to 1.5 in Fig. 7. We find that for all values of ϵ, the entropy suddenly drops at a critical point, exhibiting a sharp nonanalyticity, and therefore signifying the emergence of a different phase. The sudden drop of the entropy demonstrates either the first-order or KT phase transitions, thus excluding the second-order QPT.

With the increasing staggered biases, the flat plateau gradually changes into a broad peak and shrinks considerably at rather large ϵ. To be more clear, we replot the entropy at

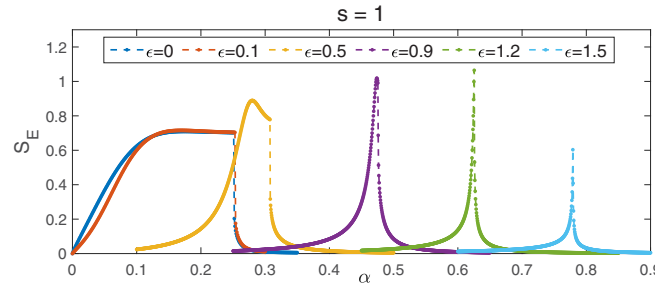

FIG. 7. Entanglement entropy S_E as a function of α in the ground state for the Ohmic bath ($s = 1$) at $\epsilon = 0, 0.1, 0.5, 0.9, 1.2, 1.5$ for $s = 1$ by VMPS approach. $\Delta = 0.1$, $\omega_c = 1$, $\Lambda = 2$, $L = 50$, $d_{\text{opt}} = 12$, and $D = 20$.

two typical staggered biases $\epsilon = 0.5$ and 0.9 in the enlarged view in the upper panels of Fig. 8. Interestingly, at $\epsilon = 0.5$, the entropy shows a broad peak before dropping abruptly at the transition point, different from that in the single SBM at $s = 1$ where the entropy saturates at a wide coupling range before a sudden drop at the transition point [35]. We argue that the coherence is lost already before the system becomes localized [32] due to the presence of the staggered biases, so the flat plateau decays to a broad peak at the finite but small ϵ. At $\epsilon = 0.9$, the maximum point of the narrow peak is very close to but still not at the transition point, in contrast to the sub-Ohmic SBM where the maximum of entanglement signifies the second-order phase transition. In these cases, the phase transition is still of KT type, as will be shown below.

To explore the possible new phase transitions of the 2SBM in the Ohmic bath driven by the large staggered bias ϵ, we also plot the entropy at rather large fields in the upper panels of Fig. 9. The entropy drops abruptly at the transition points for these large staggered biases. However, for small staggered biases in the upper panels of Fig. 8, the entropy decreases with

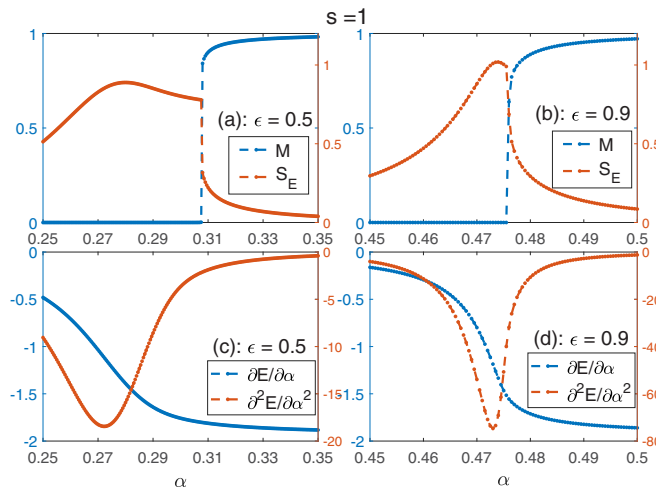

FIG. 8. Magnetization M, entanglement entropy S_E (upper panels), the first- and second-order derivatives of the ground-state energy (lower panels) as a function of α in the Ohmic bath ($s = 1$) for a weak bias $\epsilon = 0.5$ (left panels) and strong bias $\epsilon = 0.9$ (right panels), representative of the KT transition, by VMPS approach. $\Delta = 0.1$, $\omega_c = 1$, $\Lambda = 2$, $L = 50$, $d_{\text{opt}} = 12$, and $D = 20$ for $s = 1$.

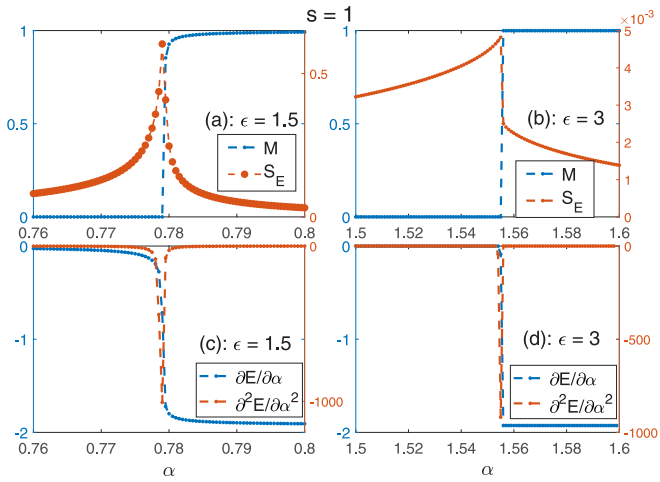

FIG. 9. Magnetization M, entanglement entropy S_E (upper panels), the first- and second-order derivatives of the ground-state energy (lower panels) as a function of α in the Ohmic bath ($s = 1$) for two strong biases $\epsilon = 1.5$ (left panels) and $\epsilon = 3$ (right panels), representative of the first-order phase transition, by VMPS approach. $\Delta = 0.1$, $\omega_c = 1$, $\Lambda = 2$, $L = 50$, $d_{\text{opt}} = 12$, and $D = 20$ for $s = 1$.

α just before the abrupt drop, contrary to the case at large staggered biases indicated in the upper panels of Fig. 9, where the entropy increases monotonically before sudden drops. The different behaviors should be originated from different kinds of phase transitions. The order parameters are then collected in the upper panels of Figs. 8 and 9. However, the order parameter jumps suddenly for all cases at the transition points, so one could not employ it to discriminate between the first-order and the KT type QPTs.

To show the nature of the phase transition in this model, we thus resort to the first-order and second-order derivatives of the ground-state energy with respect to α, as demonstrated in the low panels of Figs. 8 and 9 with the same model parameters. It is found that for small staggered biases, the first- and second-order derivatives of the ground-state energy at the transition point are continuous and do not exhibit any exotic behavior. Even the further high order derivative would not exhibit any discontinuity at the transition points, displaying the infinite-order KT phase transition nature. However, for two larger staggered biases, the first-order derivative drops suddenly, showing discontinuity at the transition point, which is just the typical characteristics of the first-order phase transition.

So in the Ohmic 2SBM with staggered biases, the KT phase transitions can be directly driven to the first-order one by increasing the staggered biases. Therefore the QuTP also exists in this model, which separates the first-order and KT critical lines. It is roughly estimated to be $\epsilon \approx 1.18$.

Finally, combining with the observations in the sub-Ohmic case in the last subsection, we can reach a conclusion that the staggered biases can drive the original QPTs to the first-order ones in 2SBM with both Ohmic and sub-Ohmic baths directly and could not change the universality of continuous phase transitions including the KT phase transitions. We believe that this conclusion can be generalized to the finite even number of dissipative spins in the staggered biases.

The universality in the QuTP in the present model is also a challenging issue. According to the Landau theory, it should be different from those in other critical points. But it is difficult to use any numerical approaches to distinguish this isolated point from others. If the analytical treatment formulated from the Feynman path-integral representation of the partition function for the single SBM [2,44–46] can be extended to this model, then it may be probable to clarify this issue.

Very interestingly, increasing the staggered biases can make the transition discontinuous in both the spin-boson model and the Dicke model [16]. It appears that there should be a common explanation for the first-order transitions in both models. There is possibly a third order term proportional to a power of the bias in the Ginzburg-Landau effective action in the Feynman path-integral representation. With increasing biases, the order parameter jumps from zero to a finite value and results in the first-order transition directly. We believe that the topic along this line deserves further careful study.

IV. CONCLUSION

We have found rich quantum phase transitions in the 2SBM with both the sub-Ohmic and the Ohmic baths in the staggered biases by the VMPS approach. The phase diagram has been composed in terms of the coupling strength and the bias magnitude. For the sub-Ohmic bath, we find that the second-order critical lines meet the first-order ones at the QuTP. For the Ohmic bath, we observe that the KT phase transitions can be driven directly to the first-order phase transitions. For all cases, if the first-order phase transition does not emerge, the universality of the phase transition could not be changed by the applied staggered biases.

The recent superconducting circuit QED system has allowed for the SBM in both the Ohmic and the sub-Ohmic bath [47–50], thus the 2SBM is experimentally feasible. Unlike the conventional cavity QED systems, the static bias of the qubit present in the circuit QED systems is ubiquitous and can be easily introduced and manipulated by an externally applied magnetic flux [51,52], which provides an additional dimension to exhibit the rich QPTs. Generalized Dicke models without the nonlinear Stark coupling undergo the second-order QPT in the thermodynamic limit (i.e., infinite atomic number $N \to \infty$) [16], while the finite-component QPT requires us to implement an extremely large detuning (i.e., infinite frequency ratio $\Delta/\omega \to \infty$) [5,9,17], so the present considered phase transition in the 2SBM in the staggered biases might be easier to realize experimentally. We believe that the 2SBM would become a potential platform to test the rich quantum criticality and the QuTP.

ACKNOWLEDGMENTS

We acknowledge useful discussions with S. Kirchner. This work is supported by the National Key Research and Development Program of China under Grant No. 2017YFA0303002 and the National Science Foundation of China under Grant No. 11834005.

[1] R. H. Dicke, Phys. Rev. **93**, 99 (1954); C. Emary and T. Brandes, Phys. Rev. E **67**, 066203 (2003); Phys. Rev. Lett. **90**, 044101 (2003); Q.-H. Chen, Y.-Y. Zhang, T. Liu, and K.-L. Wang, Phys. Rev. A **78**, 051801(R) (2008); T. Liu, Y.-Y. Zhang, Q.-H. Chen, and K.-L. Wang, *ibid.* **80**, 023810 (2009); D. Nagy and P. Domokos, Phys. Rev. Lett. **115**, 043601 (2015); Phys. Rev. A **94**, 063862 (2016).

[2] A. J. Leggett, S. Chakravarty, A. T. Dorsey, M. P. A. Fisher, A. Garg, and W. Zwerger, Rev. Mod. Phys. **59**, 1 (1987).

[3] H. P. Breuer and F. Petruccione, *The Theory of Open Quantum Systems* (Oxford University Press, New York, 2002).

[4] U. Weiss, *Quantum Dissipative Systems* (World Scientific Publishing Company, Singapore, 2008).

[5] M.-J. Hwang, R. Puebla, and M. B. Plenio, Phys. Rev. Lett. **115**, 180404 (2015).

[6] M. X. Liu, S. Chesi, Z.-J. Ying, X. S. Chen, H.-G. Luo, and H.-Q. Lin, Phys. Rev. Lett. **119**, 220601 (2017).

[7] L.-T. Shen, Z.-B. Yang, H.-Z. Wu, and S.-B. Zheng, Phys. Rev. A **95**, 013819 (2017).

[8] Z.-J. Ying, L. Cong, and X.-M. Sun, J. Phys. A: Math. Theor. **53**, 345301 (2020).

[9] S. Felicetti and A. Le Boité, Phys. Rev. Lett. **124**, 040404 (2020).

[10] Y.-F. Xie, X.-Y. Chen, X.-F. Dong, and Q.-H. Chen, Phys. Rev. A **101**, 053803 (2020); X.-Y. Chen, Y.-F. Xie, and Q.-H. Chen, *ibid.* **102**, 063721 (2020).

[11] R. Bulla, N. H. Tong, and M. Vojta, Phys. Rev. Lett. **91**, 170601 (2003); M. Vojta, N. H. Tong, and R. Bulla, *ibid.* **94**, 070604 (2005); R. Bulla, *ibid.* **102**, 249904(E) (2009).

[12] J. Ye and C. L. Zhang, Phys. Rev. A **84**, 023840 (2011).

[13] A. Baksic and C. Ciuti, Phys. Rev. Lett. **112**, 173601 (2014).

[14] J. Peng, Enrique Rico, J. X. Zhong, E. Solano, and I. L. Egusquiza, Phys. Rev. A **100**, 063820 (2019).

[15] Z. Q. Zhang, C. H. Lee, R. Kumar, K. J. Arnold, S. J. Masson, A. L. Grimsmo, A. S. Parkins, and M. D. Barrett, Phys. Rev. A **97**, 043858 (2018).

[16] Y. Xu and H. Pu, Phys. Rev. Lett. **122**, 193201 (2019).

[17] H. J. Zhu, K. Xu, and G. F. Zhang, and W. M. Liu, Phys. Rev. Lett. **125**, 050402 (2020).

[18] R. B. Griffiths, Phys. Rev. Lett. **24**, 715 (1970).

[19] A. Winter, H. Rieger, M. Vojta, and R. Bulla, Phys. Rev. Lett. **102**, 030601 (2009).

[20] A. Alvermann and H. Fehske, Phys. Rev. Lett. **102**, 150601 (2009).

[21] M. Vojta, R. Bulla, F. Güttge, and F. Anders, Phys. Rev. B **81**, 075122 (2010).

[22] Y.-Y. Zhang, Q.-H. Chen, and K.-L. Wang, Phys. Rev. B **81**, 121105(R) (2010).

[23] A. W. Chin, J. Prior, S. F. Huelga, and M. B. Plenio, Phys. Rev. Lett. **107**, 160601 (2011).

[24] C. Guo, A. Weichselbaum, J. von Delft, and M. Vojta, Phys. Rev. Lett. **108**, 160401 (2012).

[25] M. F. Frenzel and M. B. Plenio, New J. Phys. **15**, 073046 (2013).

[26] C. R. Duan, Z. F. Tang, J. S. Cao, and J. L. Wu, Phys. Rev. B **95**, 214308 (2017).

[27] S. He, L. W. Duan, and Q.-H. Chen, Phys. Rev. B **97**, 115157 (2018).

[28] N. J. Zhou, Y. Y. Zhang, Z. G. Lü, and Y. Zhao, Ann. Phys. **530**, 1800120 (2018).

[29] H. Wang and J. Shao, J. Phys. Chem. A **123**, 1882 (2019).

[30] G. De Filippis, A. de Candia, A. L. M. Cangemi, M. Sassetti, R. Fazio, and V. Cataudella, Phys. Rev. B **101**, 180408 (2020).

[31] Y.-Z. Wang, S. He, L. W. Duan, and Q.-H. Chen, Phys. Rev. B **101**, 155147 (2020).

[32] P. P. Orth, D. Roosen, W. Hofstetter, and K. Le Hur, Phys. Rev. B **82**, 144423 (2010).

[33] H. Zheng, Z. G. Lu, and Y. Zhao, Phys. Rev. E **91**, 062115 (2015).

[34] A. Winter and H. Rieger, Phys. Rev. B **90**, 224401 (2014).

[35] A. Kopp and K. Le Hur, Phys. Rev. Lett. **98**, 220401 (2007).

[36] A. W. Chin, A. Rivas, S. F. Huelga, and M. B. Plenio, J. Math. Phys. **51**, 092109 (2010).

[37] F. A. Y. N. Schröder and A. W. Chin, Phys. Rev. B **93**, 075105 (2016).

[38] A. Weichselbaum, F. Verstraete, U. Schollwöck, J. I. Cirac, and J. von Delft, Phys. Rev. B **80**, 165117 (2009).

[39] H. Saberi, A. Weichselbaum, and J. von Delft, Phys. Rev. B **78**, 035124 (2008).

[40] Y.-Z. Wang, S. He, L. W. Duan, and Q.-H. Chen, Phys. Rev. B **100**, 115106 (2019).

[41] A. Kopp, X. Jia, and S. Chakravarty, Ann. Phys. **322**, 1466 (2007).

[42] K. Le Hur, P. Doucet-Beaupre, and W. Hofstetter, Phys. Rev. Lett. **99**, 126801 (2007).

[43] M. E. Fisher, Phys. Rev. Lett. **29**, 917 (1972); E. Luijten and H. W. J. Blöte, Phys. Rev. B **56**, 8945 (1997).

[44] M. Vojta, Phys. Rev. B **85**, 115113 (2012).

[45] S. Kirchner, J. Low Temp. Phys. **161**, 282 (2010).

[46] S. Kirchner, Q. Si, and K. Ingersent, Phys. Rev. Lett. **102**, 166405 (2009); S. Kirchner, K. Ingersent, and Q. Si, Phys. Rev. B **85**, 075113 (2012).

[47] L. Magazzù, P. Forn-Díaz, R. Belyansky, J.-L. Orgiazzi, M. A. Yurtalan, M. R. Otto, A. Lupascu, C. M. Wilson, and M. Grifoni, Nat. Commun. **9**, 1403 (2018).

[48] N. Lambert, A. Shahnawaz, M. Cirio, and F. Nori, Nat. Commun. **10**, 3721 (2019).

[49] P. Forn-Díaz, J. J. García-Ripoll, B. Peropadre, J.-L. Orgiazzi, M. A. Yurtalan, R. Belyansky, C. M. Wilson, and A. Lupascu, Nat. Phys. **13**, 39 (2017).

[50] T. Yamamoto and T. Kato, J. Phys. Soc. Jpn. **88**, 094601 (2019); Y. Tokura, JPSJ News Comments **16**, 15 (2019).

[51] T. Niemczyk, F. Deppe, H. Huebl, E. P. Menzel, F. Hocke, M. J. Schwarz, J. J. Garcia-Ripoll, D. Zueco, T. Hümmer, E. Solano, A. Marx, and R. Gross, Nat. Phys. **6**, 772 (2010).

[52] F. Yoshihara, T. Fuse, S. Ashhab, K. Kakuyanagi, S. Saito, and K. Semba, Nat. Phys. **13**, 44 (2017).